Robust Multiview Registration of 3D Surfaces via ℓ_1-norm Minimization

Anil C. Raghuramu
cranil@ee.iisc.ernet.in

Department of Electrical Engineering
Indian Institute of Science
Bangalore, India

Abstract

In this paper we present a robust method for simultaneous registration of multiple 3D scans. Rigid registration is an important task in many applications such as surface reconstruction, navigation and computer aided design. The goal of 3-D (rigid) registration is to align surfaces through a (rigid) transformation. A large number of existing registration algorithms are dependent on finding matching points between scans, but a significant number of them are spurious, and it is necessary to clean up the matches obtained. This requires a substantial amount of tuning of parameters and the final result might still contain outliers. Since the number of outliers are sparse we formulate the registration optimization using the ℓ_1-norm. We present experimental results to show that the performance of our algorithm is comparable to state of the art algorithms.

1 Introduction

Registration (or alignment) of surfaces is an important task in many areas such as robotics, computer aided modeling, virtual reality and surface reconstruction. Building a full model of a object requires registering multiple surfaces observed from different viewpoints. In this paper we present an approach for registering multiple surfaces simultaneously when the transformation is rigid.

1.1 Pairwise Registration

The problem of pairwise rigid registration is to find a rigid transformation $\mathbf{M}$, that aligns two surfaces $\mathcal{S}_1$ and $\mathcal{S}_2$. This can be expressed mathematically as

$$\min_{\mathbf{M}\in SE(3)} \mathcal{E}(\mathbf{M}) = \int_{\mathbf{x}\in\mathcal{S}_1} d(\mathbf{M}\mathbf{x},\mathcal{S}_2)^2\, d\mathbf{x} \tag{1}$$

Where $\mathbf{M}$ is of the form

$$\mathbf{M} = \begin{bmatrix} \mathbf{R} & \mathbf{t} \\ \mathbf{0} & 1 \end{bmatrix} \tag{2}$$

with $\mathbf{R}$ and $\mathbf{t}$ being rotation and translation respectively, $\mathbf{x} = \begin{bmatrix} x & y & z & 1 \end{bmatrix}^T$ and $d(\mathbf{x},\mathcal{S}) = \min_{\mathbf{y}\in\mathcal{S}} ||\mathbf{x}-\mathbf{y}||_2$ is the distance of point $\mathbf{x}$ to the surface $\mathcal{S}$. When the observations are discrete

Pages 62.1-62.11
DOI: https://dx.doi.org/10.5244/C.29.62

the integral can be replaced by a summation.

$$\min_{\mathbf{M}\in SE(3)} \sum_{\mathbf{x}\in\mathcal{S}_1} d(\mathbf{M}\mathbf{x},\mathcal{S}_2)^2 \tag{3}$$

1.2 Iterative Closest Point

The iterative closest point algorithm (ICP) (Besl and McKay [5], Chen and Medioni [10]) is a pairwise alignment method which iteratively solves the optimization problem (3) by splitting the problem into a correspondence estimation step and a transformation estimation step.

Correspondence Estimation: The correspondence estimation problem is to find a point in $\mathbf{y}_i \in \mathcal{S}_2$ for each $\mathbf{x}_i \in \mathcal{S}_1$. When the scans are close enough the correspondences can be calculated using closest point queries [5] as above. If the scans are far apart correspondences can be found using feature matching with features like spin images [15] and SHOT [19]. In either case the matches are not always accurate. For instance when the scans are partially overlapping, some points in the scans will not have matching points. Hence, heuristics are applied for better alignment *e.g.* removing correspondences which are too far away; see Rusinkiewicz and Levoy [18] for more details.

Transformation Estimation: Once the correspondences are known, the transformation can be estimated by minimising a sum of squared distance function

$$\min_{\mathbf{M}\in SE(3)} \sum_{i=1}^{m} d(\mathbf{M}\mathbf{x}_i,\mathbf{y}_i)^2 \tag{4}$$

The distance function $\dot{(\mathbf{x},\mathbf{y})}$ varies based on the approximation of $d(\mathbf{x},\mathcal{S})$ used. Commonly used are the euclidean distance (or point-to-point distance) and the distance between the point $\mathbf{x}$ and the tangent plane of $\mathcal{S}$ containing $\mathbf{y}$.

The classical ICP algorithm uses the closest point to find the correspondence and the point-to-point distance for estimating the transformation

$$\text{Step (1)} \qquad \mathbf{y}_i^{k+1} = \arg\min_{\mathbf{y}\in\mathcal{S}_2} ||\mathbf{M}^k\mathbf{x}_i - \mathbf{y}||^2 \tag{5}$$

$$\text{Step (2)} \qquad \mathbf{M}^{k+1} = \arg\min_{\mathbf{M}\in SE(3)} \sum_{i=1}^{N} ||\mathbf{M}\mathbf{x}_i - \mathbf{y}_i^{k+1}||^2 \tag{6}$$

The optimization (6) can be solved using SVD [3, 21] and finding the closest point can be using the *kd*-tree [12] data structure. It can be seen that this algorithm converges to a local minimum since sequence $\mathcal{E}(\mathbf{M}^k)$ is monotonically decreasing [5].

1.3 Multiview Registration

While pairwise registration registers two scans at a time, multiview registration simultaneously registers multiple scans. Given scans $\mathcal{S}_1 \ldots \mathcal{S}_N$ and a view-graph (i.e. a graph with edges between scans which have common points), $\mathcal{G} = (\{1\ldots N\}, E)$. This problem can be generalized as

$$\min_{\mathbf{M}_i\in SE(3)} \mathcal{E}(\mathbf{M}_1\ldots\mathbf{M}_N) \tag{7}$$

Where

$$\mathcal{E}(\mathbf{M}_1 \ldots \mathbf{M}_N) = \sum_{(i,j)\in E} \sum_{\mathbf{x}\in\mathcal{S}_i} d(\mathbf{M}_i\mathbf{x}, \mathbf{M}_j\mathcal{S}_j)^2 \tag{8}$$

and $\mathbf{M}\mathcal{S} = \{\mathbf{M}\mathbf{x} \,|\, \mathbf{x} \in \mathcal{S}\}$.

1.4 Multiview ICP

Similar to pairwise registration, aligning multiple scans can also be divided into correspondence estimation and transformation estimation steps as shown in Algorithm 1.

Algorithm 1: A generic Multiview ICP algorithm.
We can replace the transformation estimation step (Line 12) with various methods discussed in later sections.

In : Scans $\mathcal{S}_1 \ldots \mathcal{S}_N$, view graph G
Out: The aligned scans $\mathcal{S}_1^* \ldots \mathcal{S}_N^*$;
Aligning transformations $\hat{\mathbf{M}}_1 \ldots \hat{\mathbf{M}}_N$

1 Initialize: $s = 0$;
2 **for** $i = 1 \ldots N$ **do**
3   $\mathcal{S}_i^{(s)} = S_i$
4 **end**
5 **repeat**
  `// Correspondence Estimation`
6   **foreach** $\{i, j\} \in E$ **do**
7   **foreach** $\mathbf{y}^k \in \mathcal{S}_i^{(s)}$ **do**
8       $\mathbf{x}_{ij}^k = \mathbf{y}^k$;
9       $\mathbf{x}_{ji}^k = \arg\min d(\mathbf{y}^k, S_j)$;
10   **end**
11   **end**
  `// Transformation Estimation`
12   $\{\mathbf{M}_i^{(s)}\} = \underset{\{\mathbf{M}_i\}\subset SE(3)^N}{\arg\min} \mathcal{E}(\mathbf{M}_1, \ldots, \mathbf{M}_N | \mathcal{S}_1, \ldots, \mathcal{S}_N)$;
  `// Update`
13   **for** $i = 1 \ldots N$ **do**
14     $\mathcal{S}_i^{(s+1)} = \mathbf{M}_i^{(s)} \mathcal{S}_i^{(s)}$;
15     $\hat{\mathbf{M}}_i = \mathbf{M}_i^{(s)} \hat{\mathbf{M}}_i$;
16   **end**
17   $s = s + 1$;
18 **until** *converged*;
19 **for** $i = 1 \ldots N$ **do**
20   $\mathcal{S}_i^* = \mathcal{S}_i^{(s)}$
21 **end**

2 Related Work

Early work in multiview registration include Chen and Medioni [10], Pulli [17], Benjamaa and Schmitt [4] and Williams and Bennamoun [22]. The method by Pulli [17] uses an incre-

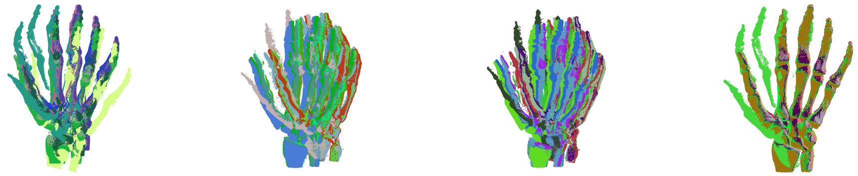

ICP initialization Torsello et al. ℓ_2-MVICP ℓ_1-MVICP

Figure 1: The results here show the performance of different algorithms when the initialization (left) is bad. Torsello et al. [20] and ℓ_2-MVICP Krishnan et al. [16] both fail while ℓ_1 MVICP ignores the outlier scan and registers the rest of them correctly.

mental method where in each step one scan is aligned with a chosen set of its neighbors. The techniques by Benjamaa and Schmitt [4] and Williams and Bennamoun [22] extend the ICP algorithm for the multiview case by solving Line 12 with the distance, d being the squared Euclidean norm the former uses a quaternion method while the latter uses a matrix based method.

More recent works include Krishnan et al. [16], Govindu and Pooja [13] and Torsello et al. [20]. Krishnan et al. [16] extend the works of Benjamaa and Schmitt [4] and Williams and Bennamoun [22] to solve Line 12 using a manifold based Newton's method. While Govindu and Pooja [13] and Torsello et al. [20] find the ICP estimates for the pairwise transformation and obtain global transformations by global averaging. They use the consistency constraint $\mathbf{M}_{ij} = \mathbf{M}_j\mathbf{M}_i$ and find the global motions by solving the minimization problem for some distance d

$$\min \sum_{i,j} d(\mathbf{M}_{ij}, \mathbf{M}_j\mathbf{M}_i)^2 \tag{9}$$

Govindu et al. exploit the Lie-algebraic nature of $SE(3)$ and use the Riemann distance for optimizing (9). Torsello et al. use the dual quaternion representation of a rigid transformation and minimize the screw distance. These methods cannot deal with cases where the obtained pairwise transformations are spurious (due to some edges being spurious.) Chatterjee et al. [9] modify the work in [13] by using a robust cost function to deal with the outlier relative motions.

3 Contribution

Since correspondences obtained are incorrect they need to be cleaned up (see [18]). This requires a tedious amount of parameter tuning and the final result might still contain outliers. Hence the need to use robust estimators. Here we present a robust framework to register point sets using the sparsity inducing ℓ_1-norm. Related work in this respect for pairwise registration can be found in Bouaziz et al. [6] and Albarelli et al. [2] for rigid registration and by Hontani et al. [14] for non-rigid registration. Bouaziz et al. [6] use ℓ_p norm and Albarelli et al. [2] use an ℓ_1 regularization for robust estimation. Our optimization problem takes an approach similar to [16] which takes into account consistency by solving for the global transformations directly. But, their cost function is susceptible to outliers. The optimization can be used for both global registration and in an ICP like method for local refinement.

4 Formulation and optimization

Robustness via sparsity imposition Consider the set of all the residual errors $\mathcal{R} = \{\mathbf{e}_{ij}\}$. A robust estimator divides the set into a small set of outliers of large magnitude and a large set of inliers with small magnitude. The ℓ_0 norm counts the number of non-zero entries we can formulate the problem as minimising $||\mathcal{R}||_0$. It has been shown that minimising ℓ_0-norm is equivalent to minimising ℓ_1 norm under certain conditions [8]. We therefore utilize the ℓ_1 norm and replace the distance in (8) by sparsity imposing ℓ_1 distance. Our registration optimization problem is

$$\mathcal{E}(\mathbf{M}_1 \ldots \mathbf{M}_N) = \sum_{(i,j)\in E} \sum_{\mathbf{x}\in\mathcal{S}_i} d_{\ell_1}(\mathbf{M}_i\mathbf{x}, \mathbf{M}_j\mathcal{S}_j) \tag{10}$$

where $d_{\ell_1}(\mathbf{x},\mathcal{S}) = \min_{\mathbf{y}\in\mathcal{S}} ||\mathbf{x}-\mathbf{y}||_1$. This can now be solved using MVICP algorithm (Algorithm 1) if the scans are close to each other. To bring them close to each other we can register pairs on a spanning tree of G (see [13] for more details) and then computing approximate values of $\mathbf{M}_i$ which will serve as a good initialization.

4.1 Correspondence estimation step

The step in line 9 of Algorithm 1 is a nearest neighbor search $\mathbf{y}^* = \arg\min_{\mathbf{y}\in\mathcal{S}} ||\mathbf{y}-\mathbf{x}||_1$. This step can be implemented by using a *kd*-tree for a ℓ_1-metric, but is slightly more expensive than ℓ_2-metric and make little difference to the algorithm. In this paper, we use the ℓ_1-metric based *kd*-tree to find correspondences.

4.2 Transformation estimation step

If we assume that the residual noise in the scans are Gaussian we can model the transformation estimation step of multiview registration problem as

$$\mathbf{e}_{ij}^k = \mathbf{M}_i\mathbf{p}_{ij}^k - \mathbf{M}_j\mathbf{p}_{ji}^k \sim \mathcal{N}(0,\sigma^2) \tag{11}$$

thus, the maximum likelihood estimate gives us ℓ_2 optimization problem which was solved by Krishnan et al. [16]. We instead formulate the problem in terms of outliers and assume that the noise is small

$$\mathbf{M}_i\mathbf{p}_{ij}^k - \mathbf{M}_j\mathbf{p}_{ji}^k = \mathbf{O}_{ij}^k \tag{12}$$

Since the vector $\mathbf{O}_{ij} = [\mathbf{O}_{ij}^{k\top} \ldots \mathbf{O}_{ij}^{n_{ij}\top}]^\top$ is sparse we can use the ℓ_1-norm to impose this constraint. So our cost function is

$$\mathcal{E}_{\ell_1}(\mathbf{M}_1 \ldots \mathbf{M}_N) = \sum_{(i,j)\in E} ||\mathbf{O}_{ij}||_1 \tag{13}$$

To solve this optimization problem, we use the Lie group structure of $SE(3)$ where, for every $\mathbf{M} \in SE(3)$ there is a unique $\mathbf{m}$ in it's corresponding Lie algebra $\mathfrak{se}(3)$ such that $\mathbf{M} = \exp(\mathbf{m})$. The matrix $\mathbf{m}$ is of the form

$$\mathbf{m} = \begin{bmatrix} \mathbf{\Omega} & \mathbf{u} \\ \mathbf{0} & 0 \end{bmatrix} \tag{14}$$

and,

$$\mathbf{\Omega} = [\boldsymbol{\omega}]_\times = \begin{bmatrix} 0 & -\omega_z & \omega_y \\ \omega_z & 0 & -\omega_x \\ -\omega_y & \omega_z & 0 \end{bmatrix} \tag{15}$$

Therefore, we can make the approximation, $\mathbf{M} = \mathbf{I} + \mathbf{m}$. The cost function can be approximated as

$$\mathbf{M}_i\mathbf{p}_{ij}^k - \mathbf{M}_j\mathbf{p}_{ji}^k \approx \mathbf{m}_i\mathbf{p}_{ij}^k - \mathbf{m}_j\mathbf{p}_{ji}^k + \delta\mathbf{p}_{ij}^k \tag{16}$$

where, $\delta\mathbf{p}_{ij}^k = \mathbf{p}_{ij}^k - \mathbf{p}_{ji}^k$. Now, let

$$\mathbf{D}_{ij} = [\cdots[\mathbf{P}_{ij}]_\times \cdots - [\mathbf{P}_{ji}]_\times \cdots - \mathbf{I}\cdots\mathbf{I}\cdots] \tag{17}$$

where,

$$[\mathbf{P}_{ij}]_\times = \begin{bmatrix} \left[\mathbf{p}_{ij}^1\right]_\times \\ \vdots \\ [\mathbf{p}_{ij}]_\times^{n_{ij}} \end{bmatrix} \tag{18}$$

Collecting all the terms we have $\mathbf{D} = [\mathbf{D}_{ij}]_{(i,j)\in E}$ and $\boldsymbol{\delta} = [\delta\mathbf{p}_{ij}^k]_{(i,j)\in E}$, the cost function is now:

$$\mathcal{E}_{\ell_1}(\mathbf{x}) = ||\boldsymbol{\delta} - \mathbf{D}\mathbf{x}||_1 \tag{19}$$

where, $\mathbf{x} = [\boldsymbol{\omega}_1 \cdots \boldsymbol{\omega}_N \; \mathbf{u}_1 \cdots \mathbf{u}_N]^T$ which can be solved iteratively (for an available implementation see [7]).

It must be noted that the approximation in (16) is valid only if $\boldsymbol{\omega}_i$'s and $\mathbf{u}_i$'s are small. Hence, the optimization cannot start from an arbitrary point. For most cases, a good starting point can be obtained by an initial pairwise ICP step. This algorithm is summarized in Algorithm 2. While this is in some sense similar to [13], we note that we estimate the global motions $\{\mathbf{M}_i\}$ directly and do not estimate the realtive motions between two scans.

Algorithm 2: Algorithm for Minimising $\mathcal{E}_{\ell_1}$

In : $\mathbf{P}_i, G, \mathbf{M}_i^0$
Out: The minimum point $\hat{\mathbf{M}}_i$
initialize $\hat{\mathbf{M}}_i := \mathbf{M}_i^0$'s;
repeat
    `// Estimate increments` $\mathbf{m}_i$ `by minimising (19)`
    Compute: $\boldsymbol{\delta}$ and $\mathbf{D}$;
    Solve: $\mathbf{x} = \arg\min_{\mathbf{x}} ||\boldsymbol{\delta} - \mathbf{D}\mathbf{x}||_1$;
    Set $\Delta\mathbf{M}_i := \exp(\mathbf{m}_i)$;
    Update $\mathbf{M}_i := \Delta\mathbf{M}_i\mathbf{M}_i$;
    Update $\mathbf{P}_i := \Delta\mathbf{M}_i\mathbf{P}_i$
until *converged*;

5 Results

In this section we present the results of robust multiview alignment method presented in the previous section. We show the performance by applying our method to both synthetic data and real world data. We first demonstrate that our estimator is indeed robust to outliers. Then we present results for some well known 3D data-sets and data acquired through the Microsoft Kinect sensor.

Evaluation of the estimator: For verifying the robustness of our cost function, we sampled 400 (these are the right correspondences) points from the Stanford bunny model. We then create five more "views" by rotating the views by an angle of $\{10°, 20°, 30°, 40°, 50°\}$ each and adding random points as outliers. The resulting error in the estimate is shown in Figure 2 for different proportions of outliers. The ℓ_2-norm based estimation method by Krishnan et al. [16] for estimating global transformations, performs poorly even when there are few outliers. In contrast the ℓ_1 method performs as expected.

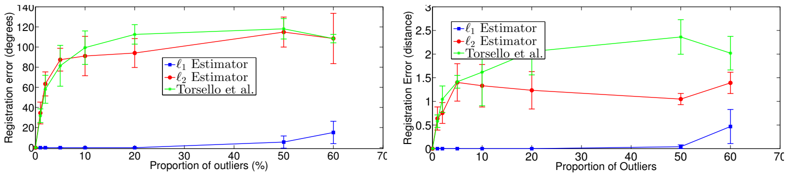

(a) Mean rotation error in degrees (b) Mean translation error

Figure 2: (a) Mean rotation error in degrees with respect to the proportion of outliers. (b) Mean translation error with respect to the proportion of outliers.
We can see clearly that our ℓ_1 estimator performs well in presence of outliers while ℓ_2 estimator fails.

Evaluation of the ℓ_1 MVICP: It can be very difficult to compare our method against all of the heuristics used in ICP since there are a large number of them, thus we will limit our comparison to heuristics that are most commonly used to remove outliers: (a) We remove all the border points from the scans; (b) the correspondences which are far away as it is done in trimmed ICP [11]; and, (c) use RANSAC to find pairwise transformations; we apply all of them to both ℓ_2-MVICP and Torsello et al. [20].

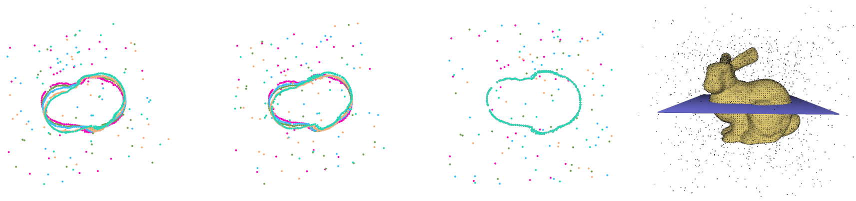

(a) Torsello et al. (b) ℓ_2-MVICP (c) ℓ_1-MVICP (d) Model

Figure 3: Results using Torsello et al. [20] (a) and ℓ_2-MVICP [16] (b) and the result of our ℓ_1-MVICP (c) Algorithm 1. As we can see ℓ_1-MVICP registers accurately while the others do not.

We demonstrate the robustness of our ICP algorithm by using the bunny model similarly as above and create five more views by rotating the models by angles of $\{10°, 20°, 30°, 40°, 50°\}$. To each of these views, we add uniform random noise to the environment (as pictured in Fig-

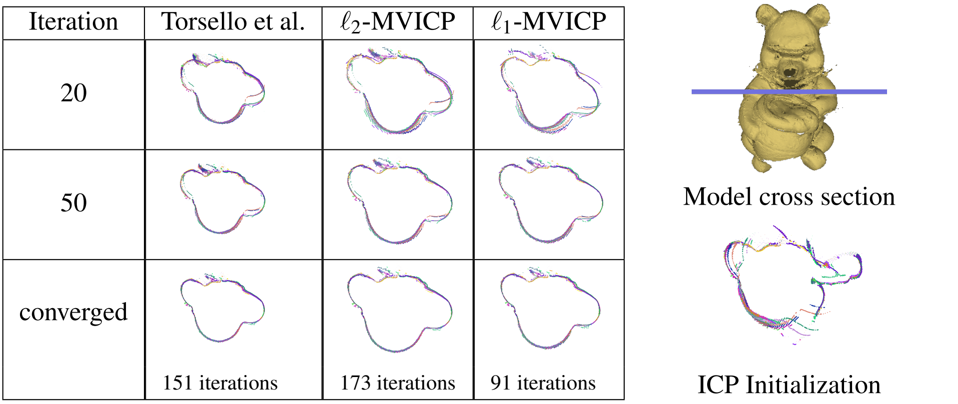

Figure 4: Result of embedding ℓ_1 estimator in Algorithm 1 on Pooh data-set from Ohio repository and comparison with ℓ_2 estimator Krishnan et al. [16] and Torsello et al. [20] at different iterations

ure 2.) In Figure 3 the performance of our algorithm is compared to ℓ_2-MVICP (where we use global optimization of Krishnan et al. [16]) and the dual quaternion diffusion of Torsello et al. [20]. We can see clearly that our method outperforms the other methods in accuracy.

For testing the algorithm on real data, we used data from the Ohio state repository [1] and a scan acquired from Microsoft Kinect. We have no good quantitative method to judge the accuracy of our algorithm since there is no ground truth. We give quantitative justifications when necessary.

Figure 1 shows a model which was initialized with poor pairwise registration. This is because one of the scans failed to register well with it's neighbors. Here, neither the method of Torsello et al. [20] nor ℓ_2 MVICP register correctly. While the proposed method fails to register the outlier the scan properly, it registers the rest of the scans well.

Figure 4 shows the cross sections of each scan for different iterations for the Pooh model. One observation we make is that by iteration 50, our method is much more closer to registration. This adds to our hypothesis of faster convergence in terms of number of iterations. Figure 5 (top) shows the results of our algorithm on the bunny model. Here too, we see that our method performs accurately compared to [13] and ℓ_2-MVICP.

Figure 5 (bottom) shows the cross-section of a model scanned using the Microsoft Kinect sensor. We give a qualitative justification by looking at how well two almost disjoint meshes which have no edge in the view graph register together. From Figure 6 (a), (b), (c) we can see that meshes in the front and sides register accurately.

6 Conclusion and future work

In this paper we presented a robust estimator for simultaneous multiview registration. We demonstrated that it performs significantly better than existing state of the art methods. For future work we intend to generalize this algorithm to use ℓ_q norms which impose an even stronger constraint on sparsity and the Huber cost function which is also shown to be robust to outliers.

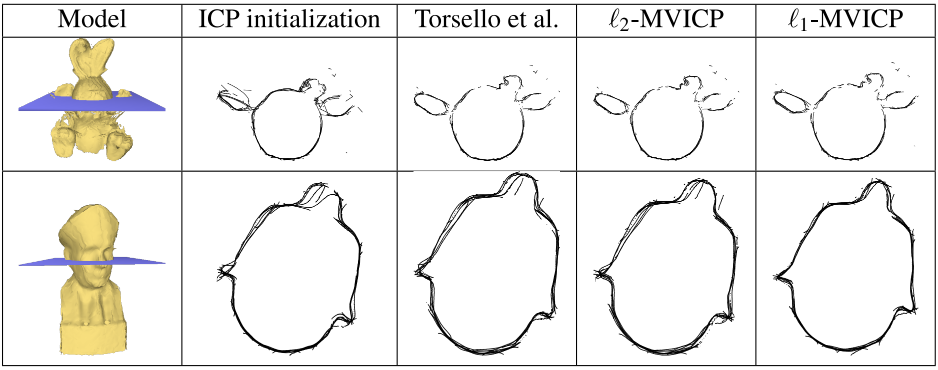

Figure 5: Top: Results for bunny model from the Ohio 3D Database. We initialize the algorithm using ICP. We see here that our ℓ_1-MVICP does as well as ℓ_2-MVICP and Torsello et al. [20]. Bottom: Results for a bust captured using Microsoft Kinect. We initialize the algorithm using ICP. We see here that both ℓ_2-MVICP and Toresllo et al. do not align the scans correctly while ℓ_1-MVICP (bottom right) does.

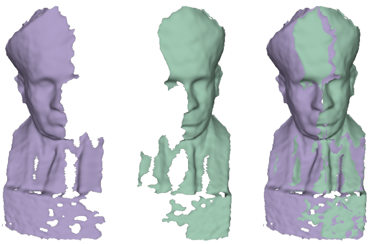

(a) Scans for the front view

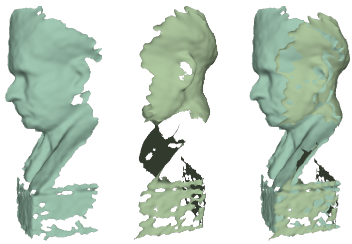

(b) Scans for the side and front view

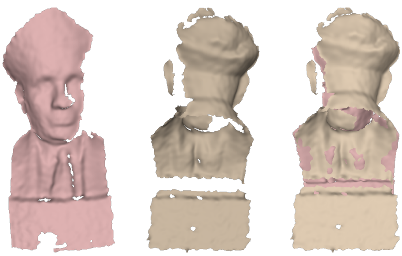

(c) Scans of the back and front views

Figure 6: Simultaneous registration of different views using our ℓ_1 MVICP method

7 Acknowledgments

This work was supported by scholarship from Ministry of Human Resource Development. The CV Raman model data was provided by Avishek Chatterjee and Venu Madhav Govindu. We thank the reviewers for their feedback.

References

[1] Ohio state university range image database. URL http://www.sampl.ece.ohio-state.edu/data/3DDB/RID/index.htm.

[2] Andrea Albarelli, Emanuele Rodola, and Andrea Torsello. A game-theoretic approach to fine surface registration without initial motion estimation. In *CVPR*, pages 430–437. IEEE, 2010.

[3] K Somani Arun, Thomas S Huang, and Steven D Blostein. Least-squares fitting of two 3-d point sets. *Pattern Analysis and Machine Intelligence, IEEE Transactions on*, (5): 698–700, 1987.

[4] R. Benjamaa and F. Schmitt. A solution for the registration of multiple 3d point sets using unit quaternions.

[5] Paul J Besl and Neil D McKay. Method for registration of 3-d shapes. In *Robotics-DL tentative*, pages 586–606. International Society for Optics and Photonics, 1992.

[6] Sofien Bouaziz, Andrea Tagliasacchi, and Mark Pauly. Sparse iterative closest point. In *Computer Graphics Forum*, volume 32, pages 113–123. Wiley Online Library, 2013.

[7] Emmanuel Candès and Justin Romberg. ℓ_1-magic: Recovery of sparse signals via convex programming. 2005. URL http://statweb.stanford.edu/~candes/l1magic/downloads/l1magic.pdf.

[8] Emmanuel J Candès, Justin Romberg, and Terence Tao. Robust uncertainty principles: Exact signal reconstruction from highly incomplete frequency information. *Information Theory, IEEE Transactions on*, 52(2):489–509, 2006.

[9] Avishek Chatterjee, Suraj Jain, and Venu Madhav Govindu. A pipeline for building 3d models using depth cameras. In *Proceedings of the Eighth Indian Conference on Computer Vision, Graphics and Image Processing*, page 38. ACM, 2012.

[10] Yang Chen and Gérard Medioni. Object modelling by registration of multiple range images. *Image Vision Comput.*, 10(3):145–155, April 1992. ISSN 0262-8856.

[11] Dmitry Chetverikov, Dmitry Stepanov, and Pavel Krsek. Robust euclidean alignment of 3d point sets: the trimmed iterative closest point algorithm. *Image and Vision Computing*, 23:299–309, 2005.

[12] J. H. Friedman, J. L. Bentley, and Finkel R. A. An algorithm for finding best matches in logarithmic expected time. *ACM Transactions on Mathematical Software (TOMS)*, pages 209–226, 1977.

[13] Venu Madhav Govindu and A. Pooja. On averaging multiview relations for 3d scan registration. *IEEE Transactions on Image Processing*, 23(3):1289–1302, March 2014. ISSN 1057-7149.

[14] Hidekata Hontani, Takamiti Matsuno, and Yoshihide Sawada. Robust nonrigid icp using outlier-sparsity regularization. In *Computer Vision and Pattern Recognition (CVPR), 2012 IEEE Conference on*, pages 174–181. IEEE, 2012.

[15] Andrew Edie Johnson. *Spin-images: a representation for 3-D surface matching*. PhD thesis, Citeseer, 1997.

[16] Shankar Krishnan, Pei Yean Lee, John B Moore, and Suresh Venkatasubramanian. Global registration of multiple 3d point sets via optimization-on-a-manifold. In *Symposium on Geometry Processing*, pages 187–196, 2005.

[17] Kari Pulli. Multiview registration for large data sets. In *Proceedings of International Conference on 3-D Digital Image Modeling*, pages 160–168, 1999.

[18] Szymon Rusinkiewicz and Marc Levoy. Efficient variants of the icp algorithm. In *3-D Digital Imaging and Modeling, 2001. Proceedings. Third International Conference on*, pages 145–152. IEEE, 2001.

[19] Federico Tombari, Samuele Salti, and Luigi Di Stefano. Unique signatures of histograms for local surface description. In *Computer Vision–ECCV 2010*, pages 356–369. Springer, 2010.

[20] Andrea Torsello, Emanuele Rodola, and Andrea Albarelli. Multiview registration via graph diffusion of dual quaternions. In *CVPR*, pages 2441–2448. IEEE, 2011.

[21] Shinji Umeyama. Least-squares estimation of transformation parameters between two point patterns. *IEEE Transactions on pattern analysis and machine intelligence*, 13(4): 376–380, 1991.

[22] J. A. Williams and M. Bennamoun. Simultaneous registration of multiple point sets using orthonormal matrices. In *IEEE International Conference on Acoustics, Speech and Signal Processing (ICASSP'2000), Istambul*, pages 2199–2202, 2000.